Ares I Flight Control System Design

Jiann-Woei Jang[1], Abran Alaniz[2], Robert Hall[3] and Nazareth Bedrossian[4]
The Charles Stark Draper Laboratory, Inc., Houston, TX, 77058

and

Charles Hall[5], Stephen Ryan[6], and Mark Jackson[7]
NASA Marshall Space Flight Center, Huntsville, AL, 35812

The Ares I launch vehicle represents a challenging flex-body structural environment for flight control system design. This paper presents a design methodology for employing numerical optimization to develop the Ares I flight control system. The design objectives include attitude tracking accuracy and robust stability with respect to rigid body dynamics, propellant slosh, and flex. Under the assumption that the Ares I time-varying dynamics and control system can be frozen over a short period of time, the flight controllers are designed to stabilize all selected frozen-time launch control systems in the presence of parametric uncertainty. Flex filters in the flight control system are designed to minimize the flex components in the error signals before they are sent to the attitude controller. To ensure adequate response to guidance command, step response specifications are introduced as constraints in the optimization problem. Imposing these constraints minimizes performance degradation caused by the addition of the flex filters. The first stage bending filter design achieves stability by adding lag to the first structural frequency to phase stabilize the first flex mode while gain stabilizing the higher modes. The upper stage bending filter design gain stabilizes all the flex bending modes. The flight control system designs provided here have been demonstrated to provide stable first and second stage control systems in both Draper Ares Stability Analysis Tool (ASAT) and the MSFC 6DOF nonlinear time domain simulation.

Nomenclature

ϕ_C = platform command angle (rad)
ϕ_P = platform angle (rad)
$\phi_{c.g.}$ = vehicle pitch angle about the center of gravity (rad)
α = angle of attack (rad)
β_E = engine gimbal angle (rad)
β_C = engine gimbal command angle (rad)
G_{GD} = engine dynamics transfer function from gimbal command to gimbal angle (unitless)
$Z_{c.g}$ = displacement of vehicle c.g. normal to reference (ft)
Z_{sj} = sloshing fluid displacement of j^{th} tank (ft)
m_{sj} = slosh mass in j^{th} tank (slug)
l_{sj} = c.g. to the j^{th} slosh-mass distance (ft)
M = total vehicle mass (slug)
c_1 = $c_{z\alpha}qA(X_{c.g.}-X_{c.p.})/I_{ZZ}$, aerodynamic acceleration coefficient (1/sec^2)

[1]Principal Member of the Technical Staff; Draper Laboratory, Houston TX, 77058: jang@draper.com, AIAA Senior Member
[2]Member of the Technical Staff; Draper Laboratory, Houston TX, 77058: aalaniz@draper.com
[3]Principal Member of the Technical Staff; Draper Laboratory, Houston TX, 77058: Robert.A.Hall@nasa.gov
[4]Group Leader, Manned Space Systems; Draper Laboratory, Houston TX, 77058: naz@draper.com
[5]Senior Aerospace Engineer; NASA Marshall Space Flight Center, Huntsville, AL 35812:Charles.E.Hall@nasa.gov
[6]Chief, Flight Mechanics and Analysis Division; NASA Marshall Space Flight Center, Huntsville, AL 35812: steve.ryan@nasa.gov
[7]Senior Aerospace Engineer; NASA Marshall Space Flight Center, Huntsville, AL 35812:Mark.E.Jackson@nasa.gov

c_2 = $FX_{c.g.}/I_{ZZ}$, vehicle angular acceleration (rad/sec^2)
I_{ZZ} = yaw vehicle moment of inertia (slug-ft^2)
$X_{c.g.}$ = center of gravity measured from the gimbal (ft)
$X_{c.p.}$ = center of pressure measured from the gimbal (ft)
S_E = engine 1st moment about gimbal (slug-ft)
I_E = engine 2nd moment about gimbal (slug-ft^2)
k_3 = $(F-D)/M$, vehicle acceleration (ft/sec^2)
k_4 = F/M, acceleration due to gimballing (ft/sec^2)
k_7 = $C_{Z\alpha}qA/M$, acceleration due to aerodynamic forces (ft/sec^2)
$C_{Z\alpha}$ = rigid-body aerodynamic side force coefficient slope (unitless)
q = dynamic pressure (lbf/ft^2)
A = reference area (ft^2)
F = gimbaled engine thrust (lbf)
V_w = cross-wind velocity (ft/sec)
V = vehicle velocity (ft/sec)
$z_{\beta i}$ = damping factor of the i^{th} bending mode (unitless)
ω_{bi} = natural frequency of the i^{th} bending mode (rad/sec)
M_i = generalized mass of the i^{th} bending mode (slug)
η_i = bending displacement of the i^{th} bending mode (ft)
$Y_{\beta i}$ = bending mode shape at gimbal (slug$^{-1/2}$)
$Y_{\beta I}'$ = bending mode slope at gimbal (slug$^{-1/2}$/ft)
$Y_{\phi i}'$ = bending mode slope at platform location (slug$^{-1/2}$/ft)
$Y_{\dot{\phi} i}'$ = bending mode slope at rate gyro location (slug$^{-1/2}$/ft)
Y_{sij} = deflection of the i^{th} bending mode at the j^{th} slosh mass location (slug$^{-1/2}$)
$C_{Z\eta i}$ = wind bending force coefficient for the i^{th} bending mode (lbf- slug$^{-1/2}$/rad)
n_b = number of bending modes
n_s = number of slosh modes (determined by number of propellant tanks)
ϕ_r = vehicle roll angle about the vehicle x-axis (rad)
$\dot{\phi}_r$ = vehicle roll rate about the vehicle x-axis (rad/s)

I. Introduction

The Ares I vehicle stack consists of a modified Shuttle heritage Solid Rocket Booster (SRB), a new upper stage being developed in-house at the Marshall Space Flight Center, the service and crew modules (Orion) managed by Johnson Space Center and a Launch Abort System solid motor extending from the top of the crew module[1]. The Ares I crew launch vehicle uses the single five-segment SRB for the first stage flight. A liquid oxygen/liquid hydrogen J-2X engine derived from the J-2 engine used on Apollo's second stage will power the second stage. Both first and second stage controls are accommodated by Thrust Vector Control (TVC) for the pitch and yaw axes and by a fixed-jet control system for the roll axis.

The Ares I vehicle has several characteristics which must be taken into account in design. First, it is aerodynamically unstable because the vehicle's center of pressure is above its center of gravity. Second, the vehicle's mass, moment of inertia, aerodynamics, slosh, and bending characteristics vary greatly throughout the launch timeline. Third, the Ares I long cylindrical body and low structural mass are sources of significant flexible body dynamics as shown in Figure 1. The large flex response in the feedback loop may cause control structure interaction and eventually result in instability if excessive control gain and incorrect phasing are presented.

To achieve desired performance and guaranteed robust stability for the Ares I control system, the flight controller design can be divided into four phases:

(1) Optimal rigid controller designs, which include phase plane controllers for roll channel and PID controllers for pitch and yaw channels. To ensure tower clearance during liftoff and minimize aerodynamic load during the Max Q region, an anti-drift/load relief controller is also included in the first stage controller design.
(2) Sensor blending selection to robustly reduce flex response in the presence of flex uncertainty[1].

(3) Flex filter designs to guarantee robust stability and adequate performance.
(4) High fidelity nonlinear simulation to verify stability and performance for entire Ares I control system.

These four design phases are not necessarily performed in sequence. For example, flex filter and controller designs can be combined into an iterative design phase.

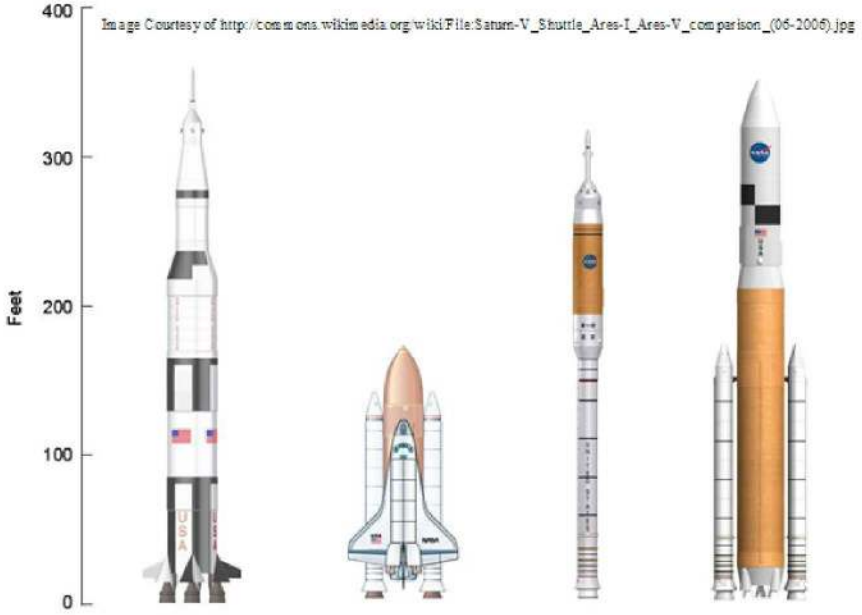

Figure 1. Saturn-V, Shuttle, Ares I, and Ares V comparison

Ascent though the dense atmosphere is the most challenge phase in the entire launching operation. The launch tower clearance and aerodynamic bending moment reduction are the most important tasks during atmospheric ascent. An optimal fly away guidance command is designed to ensure adequate clearance between the flight path and the edge of the launch tower. Moments after lift-off, an open-loop optimal guidance command steers Ares I to fly a gravitational turn to aim zero total angle of attack in a nominal trajectory[2]. The design of the TVC system is to ensure stable response to guidance commands while minimizing trajectory deviations. The TVC system gimbals the SRB engine cone to minimize both pitch and yaw attitude errors. The frequency spectrum of Ares I flight control system is shown in Figure 2. The aerodynamic forces increase significantly right after liftoff, peak at the maximum dynamic pressure region and decrease greatly afterwards; the aerodynamic effect after the first stage flight is minimal. Both flex and slosh frequencies increase over time during the entire ascent flight. Bending frequencies are much lower than torsional frequencies. Flex filters in the flight control system are designed to minimize the flex components in the error signals before they are sent to the attitude controller.

Digital filter designs and application have been extensively investigated in the literature[3-6]. The most popular analog filter design approaches include Butterworth, Chebyshev and elliptic filters. Direct digital filter design methodologies are also available in the literature[5]. These methodologies have been used for open-loop system designs by shaping filters to meet the open-loop performance specifications in the frequency domain. Unfortunately, most of the closed-loop system stability/performance requirements cannot be directly mapped into open-loop system specifications. Recently, a robust controller design methodology was proposed using a numerical constrained optimization approach to maximize stability margins while meeting performance requirements[7-11]. This control design methodology has been successfully used to design a single robust control moment gyro (CMG) flex filter set for multiple International Space Station (ISS) stages[7] and robust flex filters and a PID controller for the Orbiter Repair Maneuver operation[9].

In this paper, a design methodology for employing numerical optimization is developed for the Ares I bending filters, PID gains and anti-drift/load relief controller. The design objectives include attitude tracking accuracy, load

relief, anti-drift and robust stability with respect to rigid body dynamics, propellant slosh, and flex. Under the assumption that the Ares I time-varying dynamics and control system can be frozen over a short period of time, the bending filters are designed to stabilize all the selected frozen-time launch control systems in the presence of parametric uncertainty. Due to the large flex amplitude of the 1st bending mode and flex-slosh interaction, the first stage bending filter design achieves stability by adding lag to the first structural frequency to phase stabilize the first flex mode while gain stabilizing the higher modes. Flex amplitude of the 1st bending mode gradually decreases over time; the upper stage bending filter design is able to gain stabilize all the flex bending modes while maintaining both Ares and Orion slosh mode stability. Gain stabilization of a flexible mode refers to a filter design where the flex mode amplitude is attenuated to an extent to not cause a stability concern. Phase stabilization of a flexible mode refers to a filter design where the phasing of the first mode does not cause a stability concern. In the latter case, the control system may actively damp the structure flexure.

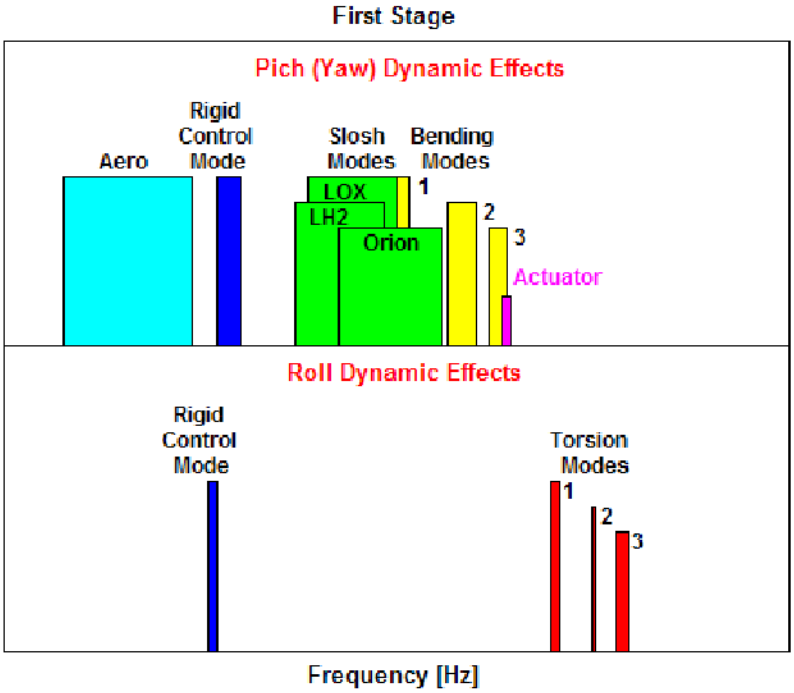

Figure 2. Ares-I First Stage Frequency Spectrum

Similarly, the first stage Roll Control System (RoCS) had to be designed to deal with disturbance torques due to vehicle dispersions in the thrust vector, center of gravity and aerodynamics while providing steering torque for roll maneuvers commanded by guidance. The upper stage reaction control system (ReCS) has to deal with transient attitude dynamics after first stage separation and upper stage engine shut down. In comparison to bending mode flex response, the torsional flex response is much lower; thus, all torsional modes are gain stabilized via filtering. After the upper stage engine cuts off, three axis control is provided by the ReCS to damp roll pitch and yaw body rates until Orion spacecraft separation. These effects had to be considered in the design of the phase planes to provide the required attitude performance while conserving propellant. A design methodology for employing numerical optimization has been developed for the Ares I torsional filter and phase plane controller.

The Ares I flight control system designs presented here have been demonstrated to provide stable first and second stage control systems in Draper Ares Stability Analysis Tool (ASAT)[3] and verified in the MSFC MAVERIC[1] (Marshall Aerospace VEhicle Representation In C) 6DOF nonlinear time domain simulation.

II. Ares-I Control System

The cross coupling effect between axes in the Ares I launch vehicle is small. This allows design and analysis to be done in each axis separately. The Ares I attitude control systems consist of both gimbal control and fixed jet

control, where the former is used for pitch and yaw control while the latter is utilized for roll control. Due to the symmetry in the pitch and yaw axis as shown in Figure 3, the TVC control system can be designed for either pitch or yaw axis[12].

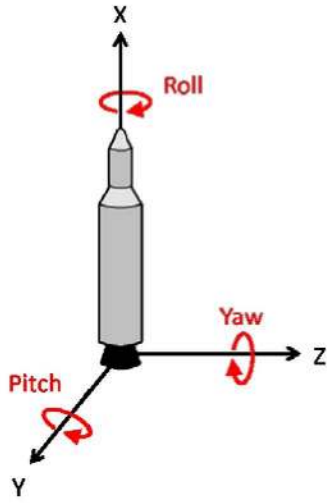

Figure 3. Spacecraft Coordinate Frame

Yaw Control System

The 2 DOF equations presented in their entirety in Reference 12-14 can be divided into rigid body dynamics, flex (bending) dynamics, and slosh dynamics. Figure 4 shows the sign conventions for the equations of motion with variables as defined in the List of Variables[12]. Note that the 2 DOF in this depiction include translation in the Y-axis and rotation in the Yaw. Rigid body dynamics includes rigid rotation about the center of gravity and the rigid body translation of the center of gravity. Specifically,

$$\phi_{c.g.}s^2 = -c_1\alpha - c_2\beta_E - \frac{1}{I_{zz}}(X_{c.g.}S_E + I_E)\beta_E s^2 + \frac{1}{I_{zz}}\sum_{j=1}^{n_s} m_{sj}(l_{sj}s^2 + k_3)Z_{sj} \quad (1)$$

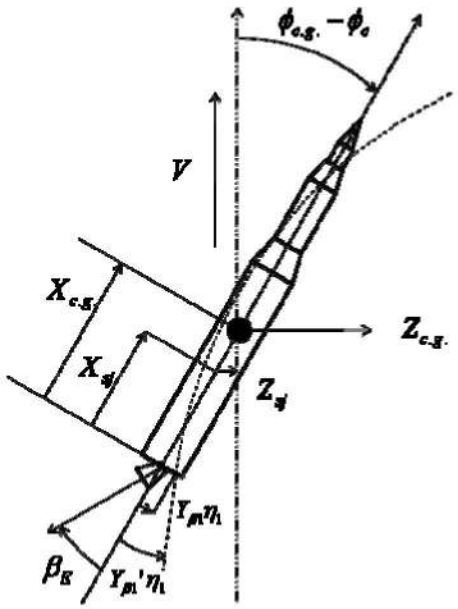

Figure 4. Spacecraft Sign Conventions

and

$$Z_{c.g.}s^2 = k_7\alpha + k_4\beta_E + k_3\phi_{c.g.} + \frac{S_E}{M}\beta_E s^2 - \frac{1}{M}\sum_{j=1}^{n_s} m_{sj}Z_{sj}s^2 \quad (2)$$

Rigid body motion depends on forces and torques created by aerodynamic pressure, gimbal angle (including the "tail-wags-dog" effect), thrust, drag, and sloshing fuel masses. Angle of attack for the undeformed vehicle is a function of wind velocity (V_w), rigid attitude ($\phi_{c.g.}$), and rigid velocity ($Z_{c.g.}s$)

$$\alpha = (V_w / V) + \phi_{c.g.} - (Z_{c.g.}s / V) \quad (3)$$

Bending motion depends on flexibility characteristics such as natural frequency, damping, and generalized mass in addition to the forces mentioned above for the rigid body dynamics. Specifically,

$$(s^2 + 2\xi_{bi}\omega_{bi}s + \omega_{bi}^2)M_i\eta_i = FY_{\beta i}\beta_E + (S_E Y_{\beta i} - I_E Y'_{\beta i})\beta_E s^2 - \sum_{j=1}^{n_s} m_{sj}Y_{sij}Z_{sj}s^2 + C_{Z\eta_i}\alpha \quad (4)$$

Each bending mode is represented by a separate equation. The inclusion of more bending modes in a model leads to an increase in model fidelity. However, this also leads to an increase in the size of the system. The number of modes included in an analysis ultimately depends on the required model fidelity, the vehicle's frequency spectrum, and the available computation tools.

The dynamics of sloshing fuel is described by an equation for each fuel tank being considered in the analysis. Specifically,

$$(s^2 + 2\xi_{sj}\omega_{sj}s + \omega_{sj}^2)Z_{sj} = -Z_{c.g.}s^2 + (l_{sj}s^2 + k_3)\phi_{c.g.} - \sum_{i=1}^{n_b} Y_{sij}\eta_i s^2 \quad (5)$$

Similar to bending modes, the inclusion of more slosh masses (up to the true number) yields a higher fidelity model. As shown in Equations 1, 2, and 4, the slosh tanks with greater slosh masses have a larger effect on overall vehicle motion. Equations 1 through 5 describe the overall yaw motion of the spacecraft and collectively form the plant dynamics.

In addition to the plant dynamics, the control system includes a combination of other systems designed to regulate the spacecraft's attitude. Sensors on the body of the vehicle determine the attitude and attitude rate according to the equations

$$\phi_P = \phi_{c.g.} + \sum_{i=1}^{n_b} Y'_{\phi i}\eta_i \quad (6)$$

and

$$\phi_{RG}s = \phi_{c.g.}s + \sum_{i=1}^{n_b} Y'_{\phi i}\eta_i s \quad (7)$$

respectively. It is apparent that sensor output only differs from plant output if bending dynamics are included in the model. Note that, when convenient, the sensor equations can be included as part of the plant's output equations. Sensor output is filtered in order to attenuate the higher frequency bending modes[3,12,13]. The filter output becomes the controller input. The controller is a proportional-integral-derivative (PID) controller that outputs a gimbal command angle

$$\beta_C = K_I\int(\phi_P - \phi_C) + K_P(\phi_P - \phi_C) + K_D\dot{\phi}_{RG} \quad (8)$$

The controller gains (K_I, K_P, and K_D) are designed using gain scheduling, a process that involves optimizing a controller for specific design points throughout the time of flight and linearly interpolating between these points to obtain gain values for any flight time [1,12]. The command angle translates the gimbal angle via the dynamics of the actuator (G_{GD})

$$\beta_E = G_{GD}\beta_C \quad (9)$$

The pitch and yaw attitude control system model as shown in Figure 5 includes the Ares-I dynamics and attitude controller modules. The Ares-I dynamics modules consist of both rigid and flex dynamics models[1,3]. The dynamics modules take in actual gimbal angles and output attitude and rate gyro measurements. The blended attitude and rate

error signals represent the difference between commanded and actual attitude and rate. They are filtered by the attitude and rate filters, respectively. The filtered error signals are sent to the PID controller as shown in Figure 5 to generate the commanded gimbal angles, which drive the gimbal dynamics. The rate blending option can be used to actively reduce structural flexibility and the attitude blending option can be used to adjust vehicle performance.

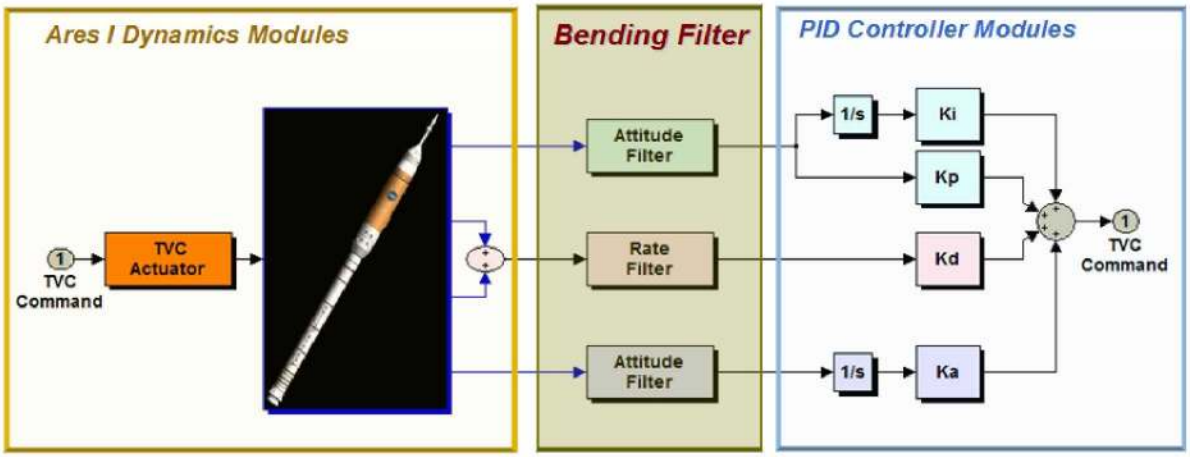

Figure 5. Ares-I Attitude Control System Model

To reduce aerodynamic load during the maximum dynamic pressure region and drifting during the liftoff, an Anti-Drift (AD) controller is added in parallel to the basic PID architecture as shown in Figure 6. The AD algorithm includes force and moment balance feedbacks using input data from rate gyros and accelerometers[1]. Signals from the AD algorithm augment those from the PID algorithm to help alleviate vehicle loading, trajectory dispersions, peak TVC deflection, and center of gravity (CG) offsets.

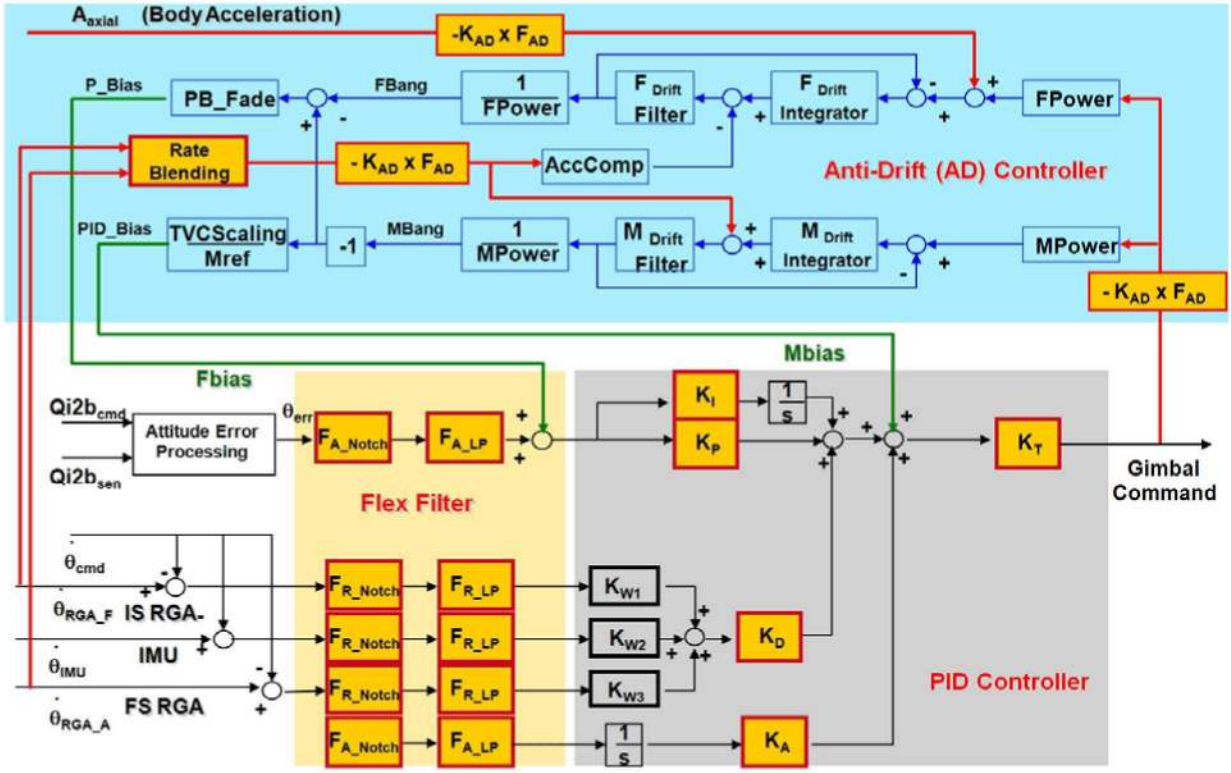

Figure 6. Ares-I Attitude and Load Relief / Anti-Drift Control System Model

Two outputs come from the AD block – a force bias term, and a moment bias term. The force bias term is used to align the thrust vector in a direction to balance external forces, and the moment bias term is an input used to balance external moments. The external forces and moments could be caused by aerodynamics, TVC offsets, gusts, winds, etc. The actual implementation includes low-pass filtering to keep noise from causing undesired results, and to keep the response frequencies of the AD low to avoid coupling with the structural vibrations. Additionally, since the accelerometer data is from the IMU, which may have a radial offset from the centerline of the vehicle and not at the axial CG location, corrections to the acceleration signals are made due to body angular rates. The AD and PID control laws require scheduled gains that are related to thrust, inertia, CG location, and weight.

Roll Control System

The ascent flight control system uses phase plane autopilots for roll attitude control during powered phases and roll, pitch, and yaw 3-axis attitude control during the post MECO coast phase of flight[1]. The roll, pitch, and yaw designs are identical, but use different data loads depending on the axis being controlled and the flight phase. Each phase plane autopilot produces a single command that takes on three states; 0 for drift, +1 for positive rotation and –1 for negative rotation. This command is sent to a jet selection logic that sets the appropriate fixed jet command(s) to "on" or "off."

Because the high-frequency flex dynamics possess the ability to make the system unstable, it is critical that a low pass filter be employed to attenuate high-frequency flex modes. The rigid and flex plant dynamics are integrated with the flex filter and phase plane controller to create the roll dynamics and control system. The block diagram in Figure 7 outlines the dynamics and control components.

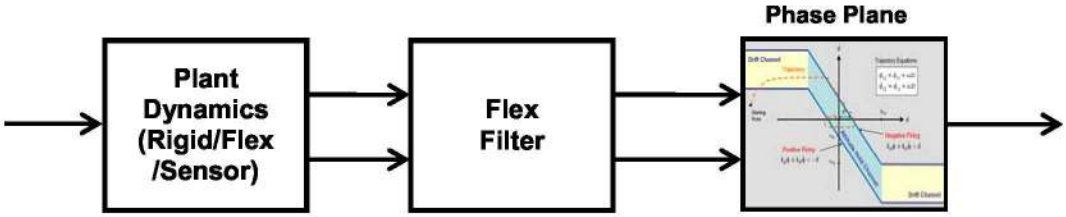

Figure 7. Ares-I Roll Control System Model

The flex filter block consists of a set of low-pass filters to attenuate high-frequency noise while at the same time allowing low-frequency dynamics to feedback into the controller. A phase plane control system regulates attitude tracking and performance. Unlike the PID controller in the TVC control system, the phase plane controller is an inherently nonlinear system which necessitates the use of nonlinear techniques in order to predict the system's behavior. The phase plane controller is "an idealized method of treating performance optimization for classes of minimum time and/or minimum fuel problems"[15]. The phase plane controller offers a unique method for attitude control while responding to the vehicle dynamics in the plane defined by state errors and state rate errors. The trajectories in the phase plane can be described through Equations 10 and 11[16].

$$\phi_{r2} = \phi_{r1} + \omega_r \Delta t \tag{10}$$

$$\dot{\phi}_{r2} = \dot{\phi}_{r1} + \alpha_r \Delta t \tag{11}$$

In the expressions above ω_r is the roll angular velocity, α_r is the roll angular acceleration and Δt is the thruster firing time for the phase plane controller.

Figure 8 shows how trajectories in the phase plane operate. For example, consider the starting point in Figure 8. The system applies a continuous torque until it enters the drift channel. At this point, the thrusters discontinue their firing and the system's attitude continues to increase because the system is in the upper half of the phase plane which means it has a positive rate. The rate is constant as long as there is no firing because the system cannot accelerate. Once the system crosses the negative switch line into the negative firing region, the system undergoes a negative acceleration which places the system back into the non-firing region; however, the system's attitude will

continue to move towards the negative firing region until the system has been driven into the lower half of the phase plane. Once there, the system's attitude will decrease in the non-firing region until it crosses the positive switch line at which point a positive firing will occur[16].

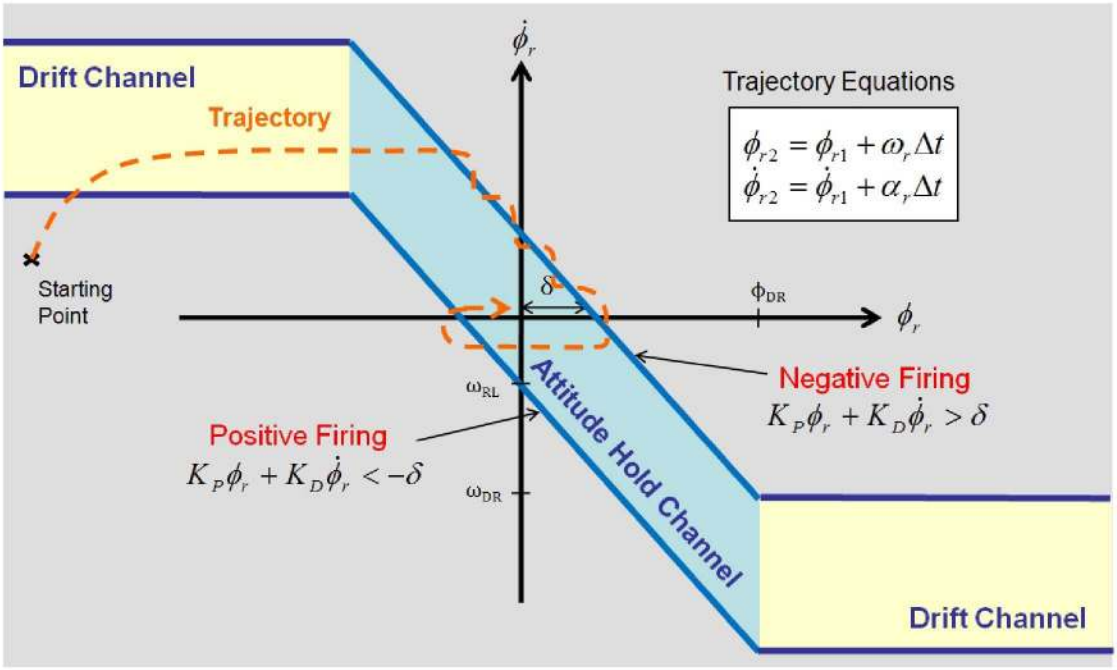

Figure 8. Simplified Ares-I Phase Plane Controller

The system will continue to oscillate around the origin of the phase plane in what is called a limit cycle. A common definition of a limit cycle is an oscillation of "fixed amplitude and fixed period without external excitation"[17]. In order to evaluate a nonlinear system such as a phase plane controlled system, it is necessary to transform the phase plane controller into a form where control techniques can be applied. This will be accomplished in a two step process. First, only the attitude hold region will be evaluated, and second, the phase plane controller will be transformed into an equivalent system consisting of a PD controller and a nonlinear element consisting of a dead zone and an ideal relay. This procedure is illustrated in Figure 9. The two switching curves in Figure 8, which define the dead zone between the positive and negative firing regions, can be defined by the inequality:

$$-(\omega_{RL}/\delta)\phi_r - \omega_{RL} < \dot{\phi}_r < -(\omega_{RL}/\delta)\phi_r + \omega_{RL} \quad (12)$$

In order to proceed from step one to step two in Figure 9, it is necessary to implement a PD controller. It is first necessary to recast Equation 12 in the form

$$-1 < \phi_r/\delta + \dot{\phi}_r/\omega_{RL} < 1 \quad (13)$$

Multiplying Equation 13 by the dead zone, δ, leads to:

$$-\delta < \phi_r + (\delta/\omega_{RL})\dot{\phi}_r < \delta \quad (14)$$

This inequality provides the following values for K_P and K_D which are the proportional and derivative gains respectively[16].

$$K_P = 1 \quad (15)$$

$$K_D = \delta/\omega_{RL} \quad (16)$$

The K_P and K_D values calculated above are critical in creating a practical phase plane controller that can be used with control analysis techniques. Substituting these values into Equation 14 yields the result for the dead zone[16].

$$-\delta < K_P\phi_r + K_D\dot{\phi}_r < \delta \quad (17)$$

It has been demonstrated in Reference 18 that with the above approximation, both Pulse-Width Modulation (PWM) and absolute stability theory can be used to predict the stability margin of a phase plane control system. The applications of both techniques have been extended to analyze and design the Ares I roll control system[18].

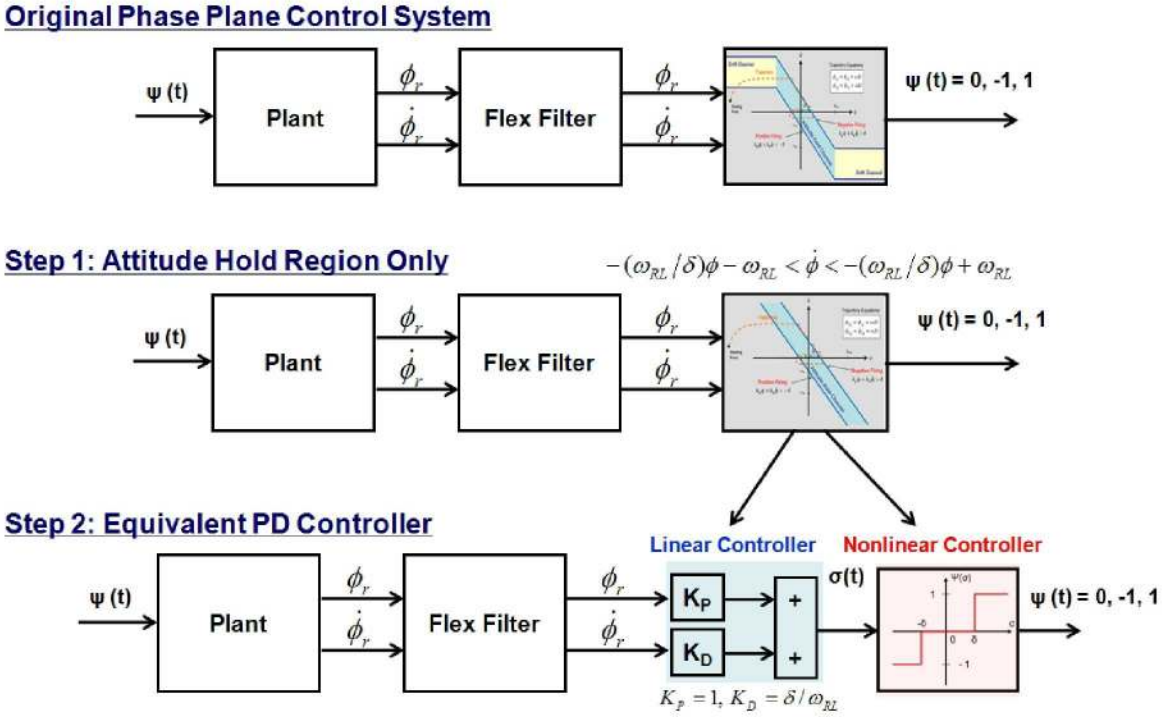

Figure 9. PD-Equivalent Phase Plane Development

III. Constrained Optimization Approach for Ares I Flight Control System Design

It has been previously demonstrated in multiple space applications[7-10] that bending filters can be designed numerically using a constrained optimization framework. The design parameters are the coefficients of the bending filters. For example, if an n^{th} order transfer function architecture is selected for both the attitude and rate filter, the total number of design parameters is 4n.

$$F_{attitude}(s) = \prod_{i=0}^{N-1} \frac{s^2 + 2x_{4*i+2}x_{4*i+1}s + x_{4*i+1}^2}{s^2 + 2x_{4*i+4}x_{4*i+3}s + x_{4*i+3}^2}$$
$$F_{rate}(s) = \prod_{i=0}^{N-1} \frac{s^2 + 2x_{4*i+2}x_{4*i+1}s + x_{4*i+1}^2}{s^2 + 2x_{4*i+4}x_{4*i+3}s + x_{4*i+3}^2} \quad \textbf{(18)}$$

In addition to filter coefficients, PID and AD controller gains/filter coefficients are also included in the design parameters set. A set of feasible parameters must satisfy the following constraints:

(C1). The filter itself must be stable and minimal phase to guarantee stability and performance.
(C2). The bandwidth of the bending filter should be greater than that of the PID controller to avoid rigid performance degradation.

These constraints can be used to set the upper and lower bounds for the bending filter design.

The primary objective of Ares-I control system design is to provide sufficient stability margins in the presence of various parameter uncertainties while maintaining adequate system response. Experience has shown that the following design objectives similar to Reference 12 are adequate:

(O1). Both nominal and perturbed closed-loop Ares-I control systems must be stable.
(O2). At least 6 dB / 30 degree rigid gain/phase margin is required for nominal control systems.

(O3). At least 3 dB / 20 degree rigid gain/phase margin is required for perturbed control systems.
(O4). At least 9 dB nominal gain margin is required for gain stabilized bending modes.
(O5). At least 45 degree nominal phase margin is required for phase stabilized bending modes.
(O6). At least 6 dB perturbed gain margin is required for gain stabilized bending modes.
(O7). At least 30 degree perturbed phase margin is required for phase stabilized bending modes.

To ensure adequate response to guidance command, attitude step response specifications are imposed in the optimization problem. The additional constraints minimize the performance degradation due to the addition of the bending filters. These attitude pointing specifications, which include requirements for rise time, percent overshoot, settling time, and steady state errors, vary during the entire flight time.

The Ares-I control systems must also ultimately demonstrate robustness to uncertainties in the plant. The goal is to design bending filters that are robust to uncertainty in structural frequency, mode shape/slope, slosh mass/ damping/frequency, vehicle mass properties, engine mass properties, aerodynamics characteristics and transportation latency. Once design objectives and constraints are identified, the bending filter design task is ready to be cast as the following constrained optimization problem

$$\begin{aligned} \min_{x} \quad & f(x) \\ s.t. \quad & \\ & g(x) \le 0 \\ & x_l \le x \le x_u \end{aligned} \tag{19}$$

The filter design criteria (C1) and (C2) can be formulated as inequality constraints. These inequality constraints can be also cast as objectives $f(x)$ in the above multi-objective constrained optimization problem. In general, these objectives are competing with each other. For example, maximizing gain margins usually diminishes phase margins. Therefore, there is no unique solution to this problem. To address this, Pareto optimality[19] must be applied to characterize the objectives. This is accomplished with a weighted sum strategy, which converts the multi-objective problem into a single objective optimization problem.

IV. Analysis of Ares I Flight Control System Design

The Ares I flight control systems consist of Thrust Vector Controller (TVC) using identical pitch/yaw autopilot architectures and a phase plane autopilot for roll control during powered flight. During the coast phase after upper stage MECO, independent roll, pitch, and yaw phase plane autopilots are used to command the US Reaction Control System (ReCS) for control. First Stage (FS) and Upper Stage (US) autopilots have the same general structure, but use different data loads such as gains, filters, limit values, and jet selection logic.

The current baseline thrust vector control law is PID with gains and filters scheduled over FS and US flight to accommodate changing flight conditions. The PID gains were designed for rigid body performance, but also to provide as much frequency separation as possible between the rigid body and expected first bending and slosh mode frequencies. For FS, the flex filters were designed to phase stabilize the first bending mode and gain stabilize higher bending modes. For US flight, the flex filters gain stabilize all bending modes. Slosh will be damped passively using mechanical baffles in the tanks, and filtering in the control system is used to supply adequate slosh gain/phase margin for gain/phase stabilized slosh modes when passive damping is inadequate for slosh gain stabilization. In FS flight, an AD (Anti-Drift) control law is added in parallel to the PID controller to actively prevent vehicle drifting into the launch tower and reduce aerodynamic load in the maximum dynamic pressure region. The AD gains and filters are also scheduled over FS flight.

The robustness of the Ares I flight control system designs are then be verified in the full Monte Carlo analysis using Draper Ares Stability Analysis Tool (ASAT) for all dispersed designated trajectories. An ASAT utility imports each nominal datum and identifies the correct flex configuration for each of a series of frozen time points. The analysis time vector is the same for each trajectory and is chosen to provide snapshots of flight with sufficient control authority (thrust magnitude) such that the stability analysis is valid. At each time point along a trajectory, 2,000 open-loop responses in both the pitch and yaw axes are computed after dispersing the relevant parameters according to a pre-generated seed vector. The seeds are consistent among axes and time points along the trajectory.

The seed vector is stored and the 2,000 open-loop responses are passed to an automated plotting and margin calculation tool. The margin calculation tool determines the characteristics of the response and tracks both the worst-case margin values and the seed identifiers that created the worst-case systems such that they can be later replicated. The following margins and characteristics are identified if they exist:

Rigid gain margin: minimum gain margin at rigid phase crossover frequencies.

Flex gain margin: negative of maximum flex peak amplitude of gain stabilized modes.

Rigid phase margin: minimum phase margin at rigid gain crossover frequency.

Flex phase margin: minimum phase margin at the flex gain crossover frequencies.

The relevant characteristics are illustrated on the Nichols response shown in Figure 10. The nominal and robust frequency margin requirements for the current design are listed in (O2) to (O7).

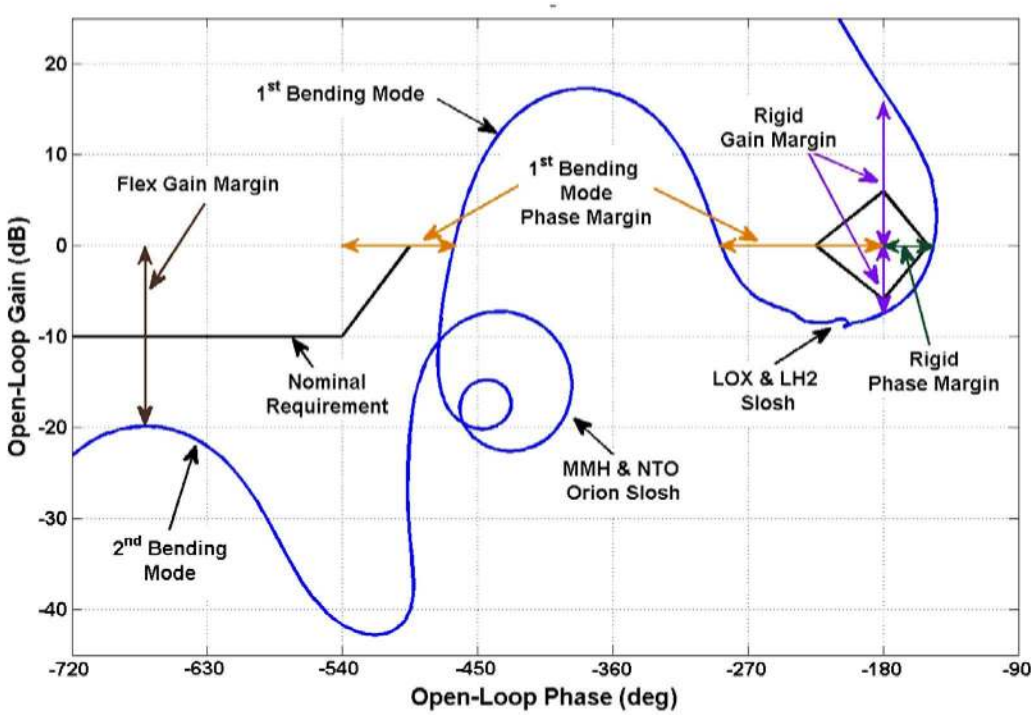

Figure 10. Stability Margin Definition Examples

In ASAT Monte Carlo analysis, frequency responses of the nominal and all dispersed control systems are depicted in both Nichols and Bode plots as shown in Figure 11. The requirements of the nominal rigid margins are indicated by the black diamond encompassing the (0 dB, -180 deg) point in the Nichols chart - the top and bottom vertices denote the rigid gain margins, and the right and left vertices indicate the rigid and flex phase margins, respectively. Similarly, the red diamond shows the rigid margin requirements for the dispersed cases. The nominal and dispersed flex gain margin requirements are drawn as black and red horizontal lines, respectively, in both Nichols and Bode plots.

V. Summary

The Ares-I launch vehicle represents a unique and challenging flex-body structural environment for control system design. This paper presents a design methodology employing numerical optimization to develop the Ares I flight control system. The flight control system design methodology was based on a numerical constrained optimization approach to maximize performance while meeting stability margins requirements. The first stage bending filter design achieves stability by adding lag to the first structural frequency and hence phase stabilizes the first Ares I flex mode while gain stabilizing the higher modes; the upper stage bending filter design gain stabilizes

all flex bending modes. The flight control system designs provided here have been demonstrated to provide stable first and second stage control systems in Draper Ares Stability Analysis Tool (ASAT).

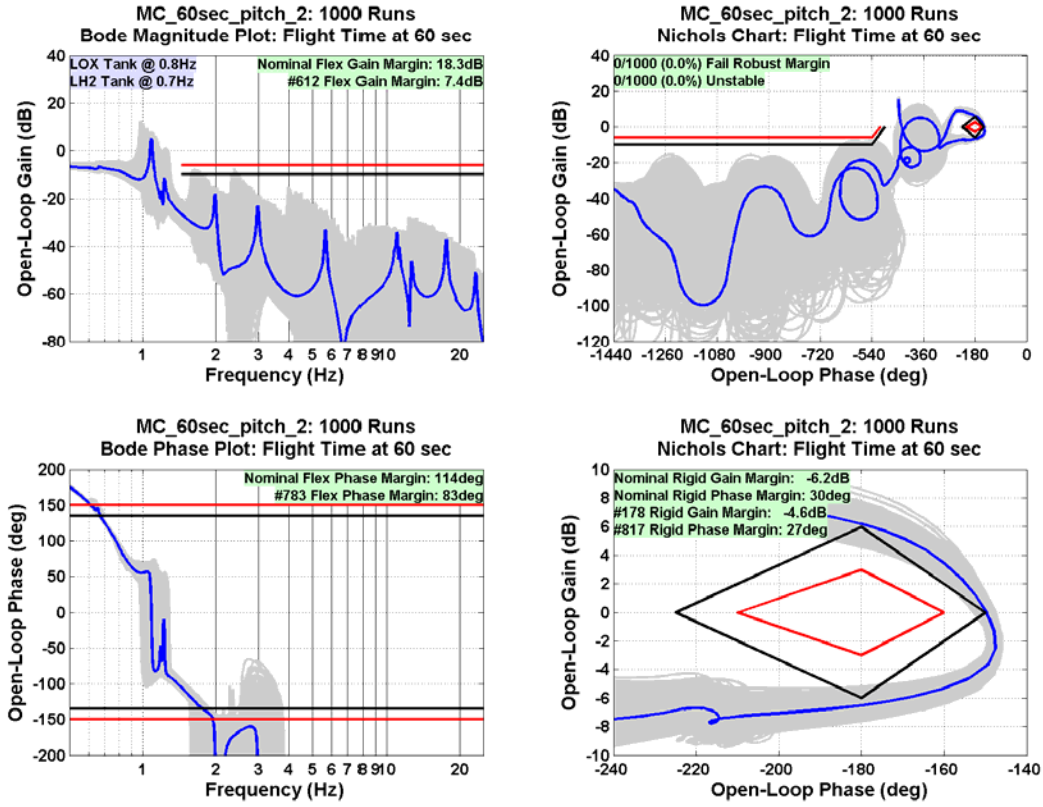

Figure 11. ASAT Monte Carlo analysis example

References

[1] Hall, C., Lee, C., Jackson, M., Whorton, M., West, M., Brandon, J., Hall, R., Jang, J., Bedrossian, N., Compton, J., and Rutherford, C., "Ares I Flight Control System Overview," AIAA GN&C Conference, Honolulu, HI, 2008, AIAA-2008-6621.

[2] Dukeman, G., "Atmospheric Ascent Guidance for Rocket-Powered Launch Vehicles", AIAA Paper 2002-4559, Proceedings of the AIAA Guidance, Navigation, and Control Conference, Monterey, CA, August 5-8, 2002.

[3] Jang, J., Hall, R., Bedrossian, N., and Hall, C., "Ares-I Bending Filter Design Using A Constrained Optimization Approach," AIAA GN&C Conference, Honolulu, HI, 2008.

[4] Oppenheim, A. V, and Schafer, R. W., Digital Signal Processing, Prentice-Hall Company, Inc., Englewood Cliffs, New Jersey, 1975.

[5] Friedlander, B., and Porat, B, "The Modified Yule-Walker Method of ARMA Spectral Estimation," IEEE Transactions on Aerospace Electronic Systems, AES-20, No. 2, March 1984, pp. 158-173.

[6] Strum, R. D. and Kirk, D. E., *First Principles of Discrete Systems and Digital Signal Processing*, Addison-Wesley Publishing Company, Inc., New York, April 1989.

[7] Jang, J., Bedrossian, N., Lee, A, Spanos, P., "A Constrained Optimization Approach for CMG Robust Flex Filter Design", AIAA GN&C Conference, August 2002.

[8] Jang, J., Lee, A., Bedrossian, N., Spanos, P., "Design of Robust Nash Game Theoretic Controllers with Time Domain Constraints," American Control Conference, 2003.

[9] Bedrossian, N., Jang, J., Alaniz, A., Johnson, M., Sebelius, K., Mesfin, Y., "International Space Station US GN&C Attitude Hold Controller Design for Orbiter Repair Maneuver," AIAA GN&C Conference, August, 2005.

[10] Postma, B., Jang, J., Bedrossian, N., Spanos, P., "Robust Constrained Optimization Approach for International Space Station Centrifuge Rotor Auto-Balancing Controller," AIAA GN&C Conference, August, 2005.

[11] Jang, J., Bedrossian, N., Hall, R., Norris, L. H., Hall, C., Jackson, M., "Initial Ares-I Bending Filter Design," 30th AAS Guidance and Control Conference, AAS 07-078, Breckenridge, Colorado, February 2007.

[12] Frosch, J.A., Vallely, D.P., "Saturn AS-501/S-IC Flight Control System Design", Journal of Spacecraft, Vol. 4, No. 8, August 1967.

[13] Haussermann, W., Duncan, R.C, "Status of Guidance and Control Methods, Instrumentation, and Techniques as Applied to the Apollo Project", Agardograph 92, NASA Code ATSS-AD, October 1964.

[14] Greensite, A. L., *Analysis and Design of Space Vehicle Flight Control Systems*, Spartan Book, New York, 1970.

[15] Penchuk, A., Hattis, P., and Kubiak, E., "A Frequency Domain Stability Analysis of a Phase Plane Control System," Journal of Guidance, Vol. 8, No. 1, 1984

[16] Wertz, J., *Spacecraft Attitude Determination and Control*, Boston, MS: D. Reidel Publishing Company, 1995.

[17] Gelb, A., and Velde, W. V., *Multiple-Input Describing Functions and Nonlinear System Design*, New York, NY: McGraw-Hill Book Co., 1968.

[18] Jang, J., Plummer, M., Bedrossian, N., Hall, C., Jackson, M., and Spanos, P., "Absolute Stability Analysis of a Phase Plane Controlled Spacecraft," 20th AAS/AIAA Space Flight Mechanics Meeting, AAS 10-112, San Diego, CA, February 2010.

[19] Rao, S. S., "Game Theory Approach for Multi-objective Structural Optimization," Computers & Structures, Vol. 24, No. 1, 1987, pp. 119-127.